Inorg. Chem. **2007**, *46*, 8071–8078

Amide–Silyl Ligand Exchanges and Equilibria among Group 4 Amide and Silyl Complexes

Hu Cai,[†,#] Xianghua Yu,[†] Shujian Chen,[†] He Qiu,[†] Ilia A. Guzei,[‡] and Zi-Ling Xue[†]

Department of Chemistry, The University of Tennessee, Knoxville, Tennessee 37996-1600, and Department of Chemistry, The University of Wisconsin, Madison, Wisconsin 53706-1396

Received May 26, 2007

$M(NMe_2)_4$ (M = Zr, **1a**; Hf, **1b**) and the silyl anion $(SiBu^tPh_2)^-$ (**2**) in $Li(THF)_2SiBu^tPh_2$ (**2**-Li) were found to undergo a ligand exchange to give $[M(NMe_2)_3(SiBu^tPh_2)_2]^-$ (M = Zr, **3a**; Hf, **3b**) and $[M(NMe_2)_5]^-$ (M = Zr, **4a**; Hf, **4b**) in THF. The reaction is reversible, leading to equilibria: 2 **1a** (or **1b**) + 2 **2** ↔ **3a** (or **3b**) + **4a** (or **4b**). In toluene, the reaction of **1a** with **2** yields $[(Me_2N)_3Zr(SiBu^tPh_2)_2]^-[Zr(NMe_2)_5Li_2(THF)_4]^+$ (**5**) as an ionic pair. The silyl anion **2** selectively attacks the $-N(SiMe_3)_2$ ligand in $(Me_2N)_3Zr-N(SiMe_3)_2$ (**6a**) to give **3a** and $[N(SiMe_3)_2]^-$ (**7**) in reversible reaction: **6a** + 2 **2** ↔ **3a** + **7**. The following equilibria have also been observed and studied: $2M(NMe_2)_4$ (**1a**; **1b**) + $[Si(SiMe_3)_3]^-$ (**8**) ↔ $(Me_2N)_3M-Si(SiMe_3)_3$ (M = Zr, **9a**; Hf, **9b**) + $[M(NMe_2)_5]^-$ (M = Zr, **4a**; Hf, **4b**); **6a** (or **6b**) + **8** ↔ **9a** (or **9b**) + $[N(SiMe_3)_2]^-$ (**7**). The current study represents rare, direct observations of reversible amide–silyl exchanges and their equilibria. Crystal structures of **5**, $(Me_2N)_3Hf-Si(SiMe_3)_3$ (**9b**), and $[Hf(NMe_2)_4]_2$ (dimer of **1b**), as well as the preparation of $(Me_2N)_3M-N(SiMe_3)_2$ (**6a**; **6b**) are also reported.

Introduction

The chemistry of transition-metal silyl complexes is of intense current interest,[1] in part, because the M−Si bonds in these complexes are very reactive. Substitution reactions have been one of primary methods to prepare transition-metal silyl complexes.[1] Replacement of a halide ligand in, for example, $(Me_2N)_3Ti-Cl$ by a silyl anion $[Si(SiMe_3)_3^-]$ is often used to yield a metal−silicon bond [in, e.g., $(Me_2N)_3TiSi(SiMe_3)_3$],[1l] and the reaction is usually *not* reversible.[1] The attack of nucleophiles on M−Si bonds was reported to cleave the M−Si bonds.[2] Reactions of $LiAlH_4$, MeLi, and RMgBr with, for example, $(OC)_4Co-SiPh_3$, afford $HSiPh_3$.[2] In the reactions involving MeLi and RMgBr, "$LiSiPh_3$" and "$BrMg-SiPh_3$", respectively, are believed to the intermediates. $LiSiPh_3$ and $BrMg-SiPh_3$ react with H_2O to give $HSiPh_3$. Transition-metal complexes are known to undergo reversible ligand exchanges[3,4] involving alkyls,[4a,b] halides,[4c,d] carbonyl,[4e] phosphines,[4f,g] amides,[4h] and cyclopentadienyls.[4i] Some exchange equilibria have been studied.

Amide−silyl exchanges have been observed and used in the preparation of main group metal silyl complexes.[5] Although reactivities of silyl ligands in transition-metal

* To whom correspondence should be addressed. E-mail: xue@ion.chem.utk.edu.

† The University of Tennessee.

‡ The University of Wisconsin.

Current address: Department of Chemistry, Nanchang University, Nanchang 336000, China.

(1) (a) Tilley, T. D. In *The Silicon−Heteroatom Bond*; Patai, S., Rappoport, Z.; Eds.; Wiley: New York, 1991; p 245 and 309. (b) Eisen, M. S. In *The Chemistry of Organic Silicon Compounds*; Rappoport, Z., Apeloig, Y., Eds.; Wiley: New York, 1998; Vol. 2, Part 3, p 2037. (c) Corey, J. Y.; Braddock-Wilking, J. *Chem. Rev.* **1999**, *99*, 175. (d) Marschner, C. *Organometallics* **2006**, *25*, 2110. (e) Shimada, S.; Tanaka, M. *Coord. Chem. Rev.* **2006**, *250*, 991. (f) Lerner, H. W. *Coord. Chem. Rev.* **2005**, *249*, 781. (g) Sharma, H. K.; Pannell, K. H. *Chem. Rev.* **1995**, *95*, 1351. (h) Yu, X.; Morton, L. A.; Xue, Z. *Organometallics* **2004**, *23*, 2210. (i) Xue, Z.-L. *Comments Inorg. Chem.* **1996**, *18*, 223. (j) Corey, J. Y. *Adv. Organomet. Chem.* **2004**, *51*, 1. (k) Gauvin, F.; Harrod, J. F.; Woo, H. G. *Adv. Organomet. Chem.* **1998**, *42*, 363. (l) Ustinov, M. V.; Bravo-Zhivotoskii, D. A.; Kalikhman, I. D.; Vitkovskii, V. Y.; Vyazankin, N. S.; Voronkov, M. G. *Organomet. Chem. USSR* **1989**, *2*, 664.

(2) (a) Colomer, E.; Corriu, R. J. P. *J. Organomet. Chem.* **1977**, *133*, 159. (b) Corriu, R. J. P.; Guerin, C. *Adv. Organomet. Chem.* **1982**, *20*, 265.

(3) (a) Moedritzer, K. *Organomet. React.* **1971**, *2*, 1. (b) Harrod, J. F. *Coord. Chem. Rev.* **2000**, *206−207*, 493. (c) Edwards, D. A. *Organomet. Chem.* **1986**, *14*, 196. (d) Lubben, T. V.; Wolczanski, P. T. *J. Am. Chem. Soc.* **1987**, *109*, 424. (e) Bryndza, H. E.; Tam, W. *Chem. Rev.* **1988**, *88*, 1163.

(4) For example, see: (a) Schaper, F.; Geyer, A.; Brintzinger, H. H. *Organometallics* **2002**, *21*, 473. (b) Poulton, J. T.; Hauger, B. E.; Kuhlman, R. L.; Caulton, K. G. *Inorg. Chem.* **1994**, *33*, 3325. (c) Fischer, H.; Seitz, F. *J. Organomet. Chem.* **1984**, *268*, 247. (d) Hunt, C. T.; Balch, A. L. *Inorg. Chem.* **1982**, *21*, 1641. (e) Palmer, G. T.; Basolo, F.; Kool, L. B.; Rausch, M. D. *J. Am. Chem. Soc.* **1986**, *108*, 4417. (f) Chisholm, M. H.; McInnes, J. M. *J. Chem. Soc., Dalton Trans.* **1997**, 2735. (g) Simms, R. W.; Drewitt, M. J.; Baird, M. C. *Organometallics* **2002**, *21*, 2958. (h) Holland, P. L.; Andersen, R. A.; Bergman, R. G.; Huang, J.; Nolan, S. P. *J. Am. Chem. Soc.* **1997**, *119*, 12800. (i) Jordan, R. F. *J. Organomet. Chem.* **1985**, *294*, 321.

10.1021/ic7010293 CCC: $37.00
Published on Web 08/21/2007

complexes have been actively investigated, there are few reports of *reversible* exchanges and equilibria involving silyl ligands.[1,3,6] We have recently studied new early transition-metal silyl complexes and their reactivities.[7] Many such silyl complexes are prepared through the replacement of halide (X^-) ligands in M−X complexes by silyl anions. In the studies of the silyl complexes, we have observed substitutions of *amide* ligands in $M(NMe_2)_4$ (M = Zr,[8,9] **1a**; Hf,[8] **1b**) and $(Me_2N)_3M-N(SiMe_3)_2$ (M = Zr, **6a**; Hf, **6b**) by silyl anions SiR_3^- [R_3 = Bu^tPh_2, **2**;[10a] $(SiMe_3)_3$, **8**[10b]] to give disilyl complexes $[M(NMe_2)_3(SiBu^tPh_2)_2]^-$ (M = Zr, **3a**; Hf, **4a**) and silyl complexes $(Me_2N)_3M-Si(SiMe_3)_3$ (M = Zr, **9a**; Hf, **9b**), respectively, through *reversible* reactions. In the reverse reactions, nucleophilic amides attack the $M-SiR_3$ bonds, leading to ligand exchange equilibria. Such substitutions of amide ligands by silyl anions and the exchange equilibria, to our knowledge, have not been reported. Our studies of the amide−silyl exchanges and thermodynamic studies of the equilibria are reported here.[11]

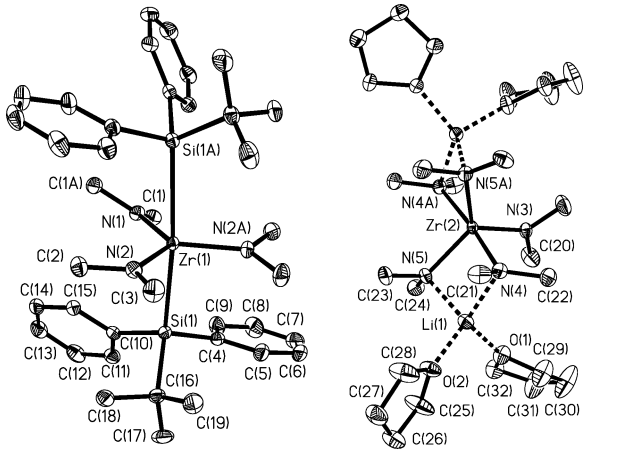

Figure 1. Molecular drawing of the anion (left) and cation (right) in **5** showing 30% probability thermal ellipsoids. The two ions are not shown in the actual mutual orientations or distances. Hydrogen atoms are omitted for clarity.

Results and Discussion

Synthesis and X-ray Structure of $[(Me_2N)_3Zr(SiBu^tPh_2)_2]^-[Zr(NMe_2)_5Li_2(THF)_4]^+$ (5). $Zr(NMe_2)_4$ (**1a**) was found to react with $Li(THF)_2SiBu^tPh_2$ (**2**-Li) in *toluene*, affording an ionic compound $[(Me_2N)_3Zr(SiBu^tPh_2)_2]^-[Zr(NMe_2)_5Li_2(THF)_4]^+$ (**5**) as a solid precipitate (eq 1). In this reaction, substitution of an amide ligand in **1a** by silyl anions leads to the formation of disilyl anion $[(Me_2N)_3Zr(SiBu^tPh_2)_2]^-$ (**3a**). The amide anion that is replaced apparently reacts with $Zr(NMe_2)_4$ (**1a**) to give the dilithium zirconium pentaamide cation $[Zr(NMe_2)_5Li_2(THF)_4]^+$ in **5** (Figure 1). Chisholm and co-workers have reported that addition of $LiNMe_2$ to $Zr(NMe_2)_4$ (**1a**) gives dilithium zirconium *hexa*amide $Zr(NMe_2)_6Li_2(THF)_2$ (**10**-Li_2).[9a] Substitution of amide ligands by aryloxide and alkoxide ligands has been reported.[12] Substitution of an amide ligand by a silyl ligand in eq 1 was unexpected. To our knowledge, this is the first known case of a replacement of an amide ligand by a silyl anion.[1]

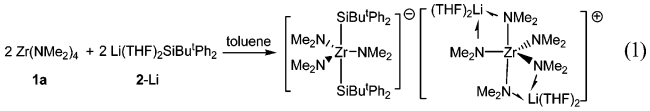

(1)

A molecular drawing, crystallographic data, and selected bond distances and angles of **5** are given in Figure 1, Table 1, and Table 2, respectively. The molecular structure of **5** consists of a discrete cation and anion pair. The anion is **3a**, and the cation consists of **4a** and two $Li(THF)_2^+$ ions. In the anion, the Zr atom is coordinated by three equatorial NMe_2 and two axial $SiBu^tPh_2$ ligands in a trigonal bipyramidal (TBP) geometry. The axial ligands are nearly staggered with respect to the equatorial NMe_2 ligands. This anionic

(5) (a) Henkel, S.; Klinkhammer, K. W.; Schwarz, W. *Angew. Chem., Int. Ed. Engl.* **1994**, *33*, 68. (b) Klinkhammer, K. W.; Schwarz, W. *Angew. Chem., Int. Ed. Engl.* **1995**, *34*, 1334. (c) Wiberg, N.; Lerner, H.-W.; Noth, H.; Ponikwar, W. *Angew. Chem., Int. Ed.* **1999**, *38*, 1103. (d) Wiberg, N.; Lerner, H.-W.; Vasisht, S.-K.; Wagner, S.; Karaghiosoff, K.; Noth, H.; Ponikwar, W. *Eur. J. Inorg. Chem.* **1999**, 1211.

(6) Alkyl (aryl),[6a−c] silenyl,[6d] silyl,[6e−h] amide,[6i] and alkoxide[6j] complexes of transition metals have been reported to undergo exchange with alkanes (arenes), silanes, amines, and alcohols through equilibria similar to the following:[6f] $Cp_2Ta(PMe_3)SiBu^t_2H + C_6H_6 \equiv [Cp_2Ta(H)(Ph)SiBu^t_2H] + PMe_3 \equiv Cp_2Ta(PMe_3)(Ph) + H_2SiBu^t_2$. For example, see: (a) Bulls, A. R.; Bercaw, J. E.; Manriquez, J. M.; Thompson, M. E. *Polyhedron* **1988**, *7*, 1409. (b) Selmeczy, A. D.; Jones, W. D.; Osman, R.; Perutz, R. N. *Organometallics* **1995**, *14*, 5677. (c) Ittel, S. D.; Tolman, C. A.; English, A. D.; Jesson, J. P. *J. Am. Chem. Soc.* **1976**, *98*, 6073. (d) Wang, W. D.; Eisenberg, R. *Organometallics* **1992**, *11*, 908. (e) Dioumaev, V. K.; Procopio, L. J.; Carroll, P. J.; Berry, D. H. *J. Am. Chem. Soc.* **2003**, *125*, 8043. (f) Jiang, Q.; Pestana, D. C.; Carroll, P. J.; Berry, D. H. *Organometallics* **1994**, *13*, 3679. (g) Nishihara, Y.; Takemura, M.; Osakada, K. *Organometallics* **2002**, *21*, 825. (h) Thorn, D. L.; Harlow, R. L. *Inorg. Chem.* **1990**, *29*, *2017*. (i) Thorman, J. L.; Guzei, I. A.; Young, V. G.; Jr.; Woo, L. K. *Inorg. Chem.* **1999**, *38*, 3814. (j) Fleischer, H.; Dienes, Y.; Schollmeyer, D. *Eur. J. Inorg. Chem.* **2002**, 2073.

(7) (a) Xue, Z.-L.; Li, L.-T.; Hoyt, L. K.; Diminnie, J. B.; Pollitte, J. L. *J. Am. Chem. Soc.* **1994**, *116*, 2169. (b) McAlexander, L. H.; Hung, M.; Li, L.-T.; Diminnie, J. B.; Xue, Z.-L.; Yap, G. P. A.; Rheingold, A. L. *Organometallics* **1996**, *15*, 5231. (c) Wu, Z.-Z.; McAlexander, L. H.; Diminnie, J. B.; Xue, Z.-L. *Organometallics* **1998**, *17*, 4853. (d) Li, L.-T.; Diminnie, J. B.; Liu, X.-Z.; Pollitte, J. L.; Xue, Z.-L. *Organometallics* **1996**, *15*, 3520. (e) Chen, T.-N.; Wu, Z.-Z.; Li, L.-T.; Sorasaenee, K. R.; Diminnie, J. B.; Pan, H.-J.; Guzei, I. A.; Rheingold, A. L.; Xue, Z.-L. *J. Am. Chem. Soc.* **1998**, *120*, 13519. (f) Wu, Z.-Z.; Diminnie, J. B.; Xue, Z.-L. *Inorg. Chem.* **1998**, *37*, 6366. (g) Choi, S.-H.; Lin, Z.-Y.; Xue, Z.-L. *Organometallics* **1999**, *18*, 5488. (h) Wu, Z.-Z.; Xue, Z.-L. *Organometallics* **2000**, *19*, 4191. (i) Wu, Z.-Z.; Diminnie, J. B.; Xue, Z.-L. *J. Am. Chem. Soc.* **1999**, *121*, 4300. (j) Wu, Z.-Z.; Diminnie, J. B.; Xue, Z.-L. *Organometallics* **1998**, *17*, 2917. (k) Wu, Z.-Z.; Cai, H.; Yu, X.-H.; Blanton, J. R.; Diminnie, J. B.; Pan, H.-J.; Xue, Z.-L. *Organometallics* **2002**, *21*, 3973. (l) Yu, X.; Bi, S.; Guzei, I. A.; Lin, Z.; Xue, Z. *Inorg. Chem.* **2004**, *43*, 7111. (m) Cai, H.; Yu, X.-H.; Chen, T.; Chen, X.-T.; You, X.-Z.; Xue, Z. *Can. J. Chem.* **2003**, *81*, 1398. (n) Qiu, H.; Cai, H.; Woods, J. B.; Wu, Z.-Z.; Chen, T.-N.; Yu, X.-H.; Xue, Z.-L. *Organometallics* **2005**, *24*, 4190. (o) Qiu, H.; Chen, S.; Xue, Z.-L. *Inorg. Chem.* **2007**, *46*, 6178.

(8) (a) Bradley, D. C.; Thomas, I. M. *J. Chem. Soc.* **1960**, 3857. (b) Chandra, G.; Lappert, M. F. *J. Chem. Soc. A* **1968**, 1940.

(9) (a) Chisholm, M. H.; Hammond, C. E.; Huffman, J. C. *Polyhedron* **1988**, *7*, 2515. (b) Diamond, G. M.; Jordan, R. F.; Petersen, J. L. *J. Am. Chem. Soc.* **1996**, *118*, 8024.

(10) (a) Campion, B. K.; Heyn, R. H.; Tilley, T. D. *Organometallics* **1993**, *12*, 2584. (b) Gutekunst, G.; Brook, A. G. *J. Organomet. Chem.* **1982**, *225*, 1.

(11) Preliminary results were published in a Communication. Yu, X.; Cai, H.; Guzei, I. A.; Xue, Z.-L. *J. Am. Chem. Soc.* **2004**, *126*, 4472.

(12) (a) Heeres, H. J.; Meetsma, A.; Teuben, J. H.; Rogers, R. D. *Organometallics* **1989**, *8*, 2637. (b) Weingarten, H.; Van Wazer, J. R. *J. Am. Chem. Soc.* **1965**, *87*, 724. (c) Wieser, U.; Babushkin, D.; Brintzinger, H.-H. *Organometallics* **2002**, *21*, 920. (d) Lappert, M. F.; Power, P. P.; Sanger, A. R.; Srivastava, R. C. *Metal and Metalloid Amide, Synthesis, Structures, and Physical and Chemical Properties*; Wiley: New York, 1980.

Table 1. Crystal Data for **5**, $(Me_2N)_3Hf-Si(SiMe_3)_3$ (**9b**) and $[Hf(NMe_2)_4]_2$

	5	**9b**	$[Hf(NMe_2)_4]_2$
empirical formula	$C_{64}H_{118}Li_2N_8O_2Si_2Zr_2$	$C_{15}H_{45}HfN_3Si_4$	$C_{16}H_{48}Hf_2N_8$
fw	1316.18	558.38	709.60
cryst syst	monoclinic	rhombohedral	monoclinic
space group	*C*2/c	*R*3c	*C2/c*
unit cell dimensions	$a = 25.145(3)$ Å $b = 17.770(3)$ Å $c = 16.346(3)$ Å $\beta = 97.789(3)°$	$a = b = 15.483(5)$ Å $c = 19.378(8)$ Å $\gamma = 120°$	$a = 20.429(13)$ Å $b = 8.454(5)$ Å $c = 15.971(10)$ Å $\beta = 112.425(10)°$
vol	7236(2) Å^3	4023(2) Å^3	2550(3) Å^3
Z	4	6	4
density (calcd)	1.208 g/cm^3	1.383 g/cm^3	1.849 g/cm^3
abs coeff	0.368 mm^{-1}	4.072 mm^{-1}	8.153 mm^{-1}
F(000)	2816	1704	1376
cryst size	0.40 × 0.25 × 0.25 mm^3	0.45 × 0.40 × 0.15 mm^3	0.55 × 0.45 × 0.07 mm^3
θ range for data collection	1.41−28.28°	2.59−28.35°	2.16−22.50°
index ranges	$-32 \le h \le 33$, $-23 \le k \le 23$, $-21 \le l \le 21$	$-20 \le h \le 19$, $-19 \le k \le 20$, $-25 \le l \le 25$	$-21 \le h \le 21$, $-9 \le k \le 9$, $-17 \le l \le 17$
reflns collected	36 482	11 001	6107
independent reflns	8684 [*R*(int) = 0.0543]	2027 [*R*(int) = 0.0348]	1628 [*R*(int) = 0.0352]
completeness	96.5% to $\theta = 28.28°$	94.5% to $\theta = 28.35°$	97.7% to $\theta = 22.50°$
max and min transm	0.9136 and 0.8667	0.5803 and 0.2616	0.5991 and 0.0940
refinement method		full-matrix least-squares on F^2	
data/restraints/params	8684/0/383	2027/1/75	1628/0/126
GOF on F^2	1.041	1.178	1.014
Final R indices	R1 = 0.0396,	R1 = 0.0490,	R1 = 0.0358,
[$I > 2\sigma(I)$]	wR2 = 0.1030	wR2 = 0.1350	wR2 = 0.0967
R indices	R1 = 0.0567,	R1 = 0.0567,	R1 = 0.0369,
(all data)	wR2 = 0.1169	wR2 = 0.1655	wR2 = 0.1000
largest diff. peak and hole	0.875 and −0.464 e Å^{-3}	2.792 and −1.690 e Å^{-3}	2.154 and −2.286 e Å^{-3}

[a] $wR2 = [\sum w(F_o^2 - F_c^2)^2/\sum w(F_o^2)^2]^{1/2}$. $R1 = \sum||F_o| - |F_c||/\sum|F_o|$; $w = 1/[\sigma^2(F_o^2) + (aP)^2 + bP]$; $P = [2F_c^2 + \max(F_o^2, 0)]/3$.

Table 2. Selected Bond Distances (Å) and Angles (deg) for **5**

Zr(1)−N(1)	2.080(2)	Zr(2)−N(4)	2.243(2)
Zr(1)−N(2)	2.0488(19)	Zr(2)−N(5)	2.1337(19)
Zr(1)−Si(1)	2.9507(7)	N(4)−Li(1)	2.099(4)
N(1)−C(1)	1.447(3)	N(5)−Li(1)	2.117(5)
N(2)−C(2)	1.442(3)	N(3)−C(20)	1.440(3)
N(2)−C(3)	1.452(3)	N(4)−C(21)	1.454(3)
Si(1)−C(4)	1.920(2)	N(4)−C(22)	1.459(3)
Si(1)−C(10)	1.926(2)	N(5)−C(23)	1.465(3)
Si(1)−C(16)	1.965(2)	N(5)−C(24)	1.459(3)
Zr(2)−N(3)	2.036(3)		
Si(1A)−Zr(1)−Si(1)	170.47(3)	N(4)−Zr(2)−N(4A)	172.54(11)
N(2)−Zr(1)−N(2A)	118.86(11)	N(5)−Zr(2)−N(5A)	124.30(11)
N(2)−Zr(1)−N(1)	120.57(6)	N(5)−Zr(2)−N(4)	85.54(8)
N(2)−Zr(1)−Si(1A)	89.83(6)	N(3)−Zr(2)−N(5)	117.85(5)
N(2)−Zr(1)−Si(1)	95.01(6)	N(3)−Zr(2)−N(4)	93.73(5)
N(1)−Zr(1)−Si(1)	85.235(13)	N(5A)−Zr(2)−N(4)	90.97(8)

disilyl complex was first observed in $[Li(THF)_4][(Me_2N)_3Zr(SiBu^tPh_2)_2]$ (**3a**-Li),[7i] which was prepared from the reaction of $(Me_2N)_3Zr-SiBu^tPh_2$ (**11a**) with $Li(THF)_3SiBu^tPh_2$ (**2**-Li). $[(Me_2N)_3Zr(SiBu^tPh_2)_2]^-$ (**3a**) represents the first isolated and structurally characterized d^0 disilyl complex free of anionic π-ligands and a rare example of a pentacoordinated d^0 Zr(IV) complex. Another reported pentacoordinated homoleptic anionic complex $[Li(dme)_3][Zr(SCMe_3)_5]$ (dme = dimethoxyethane) adopts a distorted TBP structure.[13] The *trans* angle Si−Zr−Si [170.47(3)] in **5** is near 180°, and it is slightly smaller than 177.93(5)° in $[Li(THF)_4][(Me_2N)_3Zr(SiBu^tPh_2)_2]$ (**3a**-Li).[7i] The Zr−Si bond distance of 2.9507(7) Å in **5** is close to that [2.9331(14) Å] in **3a**-Li, and it represents, to our knowledge, the longest reported Zr−Si bond.[14] Other known Zr−Si bond lengths are in the range of 2.721(2)−2.8771(10) Å.[14] This is perhaps mainly the result of the strong *trans*-influence of silyl groups in $[(Me_2N)_3Zr(SiBu^tPh_2)_2]^-$ in **5**. For late transition-metal complexes, silyl ligands are among the ligands with the strongest *trans* influence.[15] Zr−N bonds in $[(Me_2N)_3Zr(SiBu^tPh_2)_2]^-$ [2.0488(19)−2.080(2) Å in **5**; 2.039(3)−2.063(5) Å in **3a**-Li] are slightly longer than those in $(Me_2N)_3Zr-SiBu^tPh_2$ [**11a**, 2.021(4) Å] and $(Me_2N)_3Zr-Si(SiMe_3)_3$ [**9a**, 2.018(7) Å],[7f] suggesting that steric factors might play a role in the Zr−Si elongation in the disilyl anion $[(Me_2N)_3Zr(SiBu^tPh_2)_2]^-$ (**3a**). TBP complexes often show elongation of the bonds between the central metals and the axial ligands. Similar to the ZrN_5 moiety in the structure of $[Zr(NMe_2)_4]_2$,[9a] the cation in **5** reveals a distorted TBP structure around Zr(2) with the N(4) and N(4A) atoms in the axial positions. In comparison, the ZrN_6 moiety in $Zr(NMe_2)_6Li_2(THF)_2$ (**10**-Li_2) approaches an octahedron.[9a] The Zr(2)-terminal N(3) bond [2.036(2) Å] in

(13) Kawaguchi, H.; Tatsumi, K.; Cramer, R. E. *Inorg. Chem.* **1996**, *35*, 4391.

(14) Other known Zr−Si bond lengths: 2.803(2) Å in $(Me_2N)_3Zr-SiBu^tPh_2$ (**11a**),[7f] 2.781(2) Å in $(Me_2N)_3Zr-Si(SiMe_3)_3$ (**9a**),[7f] 2.860(2) Å in $(Me_2N)_2[(Me_3Si)_2N]Zr-SiBu^tPh_2$,[7f] 2.753(4) Å in $(Bu^tO)_3Zr-Si(SiMe_3)_3$ [Heyn, R. H.; Tilley, T. D. *Inorg. Chem.* **1989**, *28*, 1768], 2.848(3) Å in $(Me_3SiO)_2Zr(SiBu^tPh_2)(Cl)(THF)_2$,[7j] 2.74(2) Å in $(Bu^t-CH_2)_3Zr-Si(SiMe_3)_3$,[7c] 2.772(4) Å in $Cp_2Zr[Si(SnMe_3)_3]Cl$,[1a] 2.721(2) Å in $Cp_2Zr(SiPh_3)(H)(PMe_3)$ [Kreutzer, K. A.; Fisher, R. A.; Davis, W. M.; Buchwald, S. L. *Organometallics* **1991**, *10*, 4031], 2.813(2) Å in $Cp_2Zr(SiPh_3)Cl$ [Muir, K. *J. Chem. Soc. A* **1971**, 2663], $Cp_2Zr(SiMe_3)(S_2CNEt_2)$ [Tilley, T. D. *Organometallics* **1985**, *4*, 1452], 2.853(2) Å in $Cp_2Zr(Cl)[Si(SiMe_3)_2SiMe_2CMe_2CHMe_2]$, 2.8771(10) Å in highly crowded $Cp_2Zr[Si(SiMe_3)_3]_2$ [Kayser, C.; Frank, D.; Baumgartner, J.; Marschner, C. *J. Organomet. Chem.* **2003**, *667*, 149], and 2.866(2)−2.887(2) Å in $K(18\text{-crown-}6)_{3/2}\{(Me_2N)_3Zr[\eta^2\text{-}(Me_3Si)_2Si(CH_2)_2Si(SiMe_3)_2]\}$.[7n]

(15) Appleton, T. G.; Clark, H. C.; Manzer, L. E. *Coord. Chem. Rev.* **1973**, *10*, 355.

Table 3. Equilibrium Constants in eqs 2 and 4

T (K)	eq 2 (Zr)[a] $K_{eq}(\sigma K_{eq(ran)})$	eq 2 (Hf)[a] $K_{eq}(\sigma K_{eq(ran)})$	eq 4[a] $K_{eq}(\sigma K_{eq(ran)})$
308(1)	6.76(8)	1.6(4)	
303(1)	7.93(6)	2.1(5)	3.77(5)
298(1)	10.4(1)	2.5(8)	4.00(4)
293(1)	12.9(1)	2.8(5)	4.14(5)
288(1)	16.7(1)	3.5(5)	4.392(15)
283(1)	22.0(1)	4.3(3)	4.684(14)
278(1)	27.9(1)	5.6(2)	4.97(6)
273(1)	40.8(1)	7.5(5)	5.29(3)
268(1)	53.9(1)	8.92(16)	5.51(5)
263(1)	72.4(1)	9.62(5)	5.647(8)
258(1)	95.7(1)	11.8(1)	6.13(3)
253(1)	125(1)	13.7(5)	6.45(2)
248(1)	166(1)	16.4(1)	6.90(2)
243(1)	242(1)	18.9(10)	7.27(1)
238(1)			7.99(2)
233(1)			8.51(1)
228(1)			9.28(1)
223(1)			10.0(1)

[a] The largest random uncertainties are $\sigma K_{eq(ran)}/K_{eq} = 0.08/6.76 = 1.2\%$, $0.8/2.5 = 32\%$, and $0.05/3.77 = 1.2\%$ for eq 2 (Zr), eq 2 (Hf), and eq 4, respectively. The total uncertainties $\sigma K_{eq}/K_{eq}$ of 5.1, 32, and 5.1%, respectively, were calculated from the $\sigma K_{eq(ran)}/K_{eq}$ and the estimated systematic uncertainty $\sigma K_{eq(sys)}/K_{eq} = 5\%$ by $\sigma K_{eq}/K_{eq} = [(\sigma K_{eq(ran)}/K_{eq})^2 + (\sigma K_{eq(sys)}/K_{eq})^2]^{1/2}$.

5 is shorter than the Zr(2)-bridging N(5) bond [2.1337(19) Å]. This is consistent with less d−p π-bond character between Zr(2) and N(5), as a result of bonding between N(5) and Li(1). The Zr-terminal N lengths in **5** [2.036(3)−2.080(2) Å] are similar to those in $[Zr(NMe_2)_4]_2$ [2.050(5)-2.104(5) Å].[9a]

Amide−Silyl Exchanges Involving the $(SiBu^tPh_2)^-$ (2) Anion. When crystals of **5** were dissolved in THF-d_8, the reverse reaction in eq 1 was observed in ^{1}H and ^{13}C NMR spectra of the solution, yielding $Zr(NMe_2)_4$ (**1a**) and $(SiBu^tPh_2)^-$ (**2**).[16] In fact, $[(Me_2N)_3Zr(SiBu^tPh_2)_2]^-$ (**3a**), $[Zr(NMe_2)_5]^-$ (**4a**), **1a**, and **2** in the solution of **5** were found to be in an equilibrium in eq 2. This equilibrium was also observed when **1a** and **2** were mixed in THF-d_8. ^{1}H EXSY spectrum (t_{mix} = 2 s) of a mixture of **1a** and **2** at 32 °C is given in the Supporting Information. Strong cross-peaks were observed among three −N*Me*$_2$ peaks and between two −Si*Bu*^{t}Ph$_2$ peaks, indicating a chemical exchange process for the complexes in eq 2.

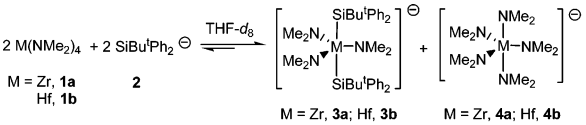

(2)

$$K_{eq} = \frac{[\,\mathbf{3a\text{-}b}\,][\,\mathbf{4a\text{-}b}\,]}{[\,\mathbf{1a\text{-}b}\,]^2\,[\,\mathbf{2}\,]^2}$$

Variable-temperature ^{1}H NMR spectroscopy over a 65 K range (243−308 K) was used to study the equilibria in THF-d_8. The equilibrium constants K_{eq} range from 242(1) at 243 K to 6.76(8) at 308 K (Table 3) for the Zr complexes, indicating that the forward reaction to give disilyl **3a** and pentaamide **4a** is favored and that decreasing the temperature shifts the equilibrium toward **3a** and **4a**. A plot of ln K_{eq} versus 1000/T by the van't Hoff equation[17] (correlation coefficient $R = 0.999$) gives the thermodynamic parameters of the equilibrium: $\Delta H° = -8.3(2)$ kcal/mol, $\Delta S° = -23.2(9)$ eu, and $\Delta G°_{298\ K} = -1.4(5)$ kcal/mol at 298 K. The forward reaction is endothermic, and the entropy change $\Delta S° = -23.3(9)$ eu reflects the stoichiometry of the reaction. The enthalpy change outweighs the entropy change in the forward reaction to give $\Delta G°_{298\ K} < 0$ in favor of **3a** and **4a**.

In toluene-d_8, an equilibrium involving $Zr(NMe_2)_4$ (**1a**), $(SiBu^tPh_2)^-$ (**2**), **3a**, **4a**, and $[Zr(NMe_2)_6]^{2-}$ (**10**) was observed. The ^{1}H NMR peaks of the amide ligands (−NMe_2) in **3a**, **4a**, **1a**, and **10** were severely overlapped, preventing accurate quantitative studies of the equilibrium. The freezing point depression studies of $[(Me_2N)_3Zr(SiBu^tPh_2)_2]^-[Zr(NMe_2)_5Li_2(THF)_4]^+$ (**5**) in benzene suggest that dissolution of 1 equiv of **5** in benzene generates ~3 equiv of neutral or ionic species. This is consistent with the fact that, in solution, **5** is involved in an equilibrium that gives several additional species including **3a**, **4a**, $Zr(NMe_2)_4$ (**1a**), $[Li(THF)_n]^+$, $(SiBu^tPh_2)^-$ (**2**), and $[Zr(NMe_2)_6]^{2-}$ (**10**).

The reaction between $Hf(NMe_2)_4$ (**1b**) and $Li(THF)_2SiBu^tPh_2$ (**2**-Li) gives an equilibrium similar that of Zr analog (eq 2). Overlaps of the ^{1}H NMR resonances of the −N*Me*$_2$ ligands in both THF-d_8 and toluene-d_8 were observed, leading to larger errors in the measurement of K_{eq} values listed in Table 3. A plot of ln K_{eq} versus 1000/T (correlation coefficient $R = 0.982$) yields $\Delta H° = -5.7(10)$ kcal/mol, $\Delta S° = -17(4)$ eu, and $\Delta G°_{298\ K} = -0.6(20)$ kcal/mol at 298 K for the equilibrium of the Hf complexes in THF-d_8.[17] These thermodynamic parameters are similar to those of their Zr analogs discussed earlier.

We reported earlier that the disilyl anions $[(Me_2N)_3M(SiBu^tPh_2)_2]^-$ (M = Zr, **3a**; Hf, **3b**) undergo silyl−silyl exchanges in eq 3.[7i,n] NMR studies of $Zr(NMe_2)_6Li_2(THF)_2$ (**10**-Li_2) by Chisholm and co-workers suggest that $LiNMe_2$ dissociates from **10**-Li_2.[9a] These silyl and amide dissociations may be present in the reactions in eq 2. NMe_2^- dissociated from $[M(NMe_2)_5]^-$ (**4a**) subsequently attacks the M−Si bonds in $[M(NMe_2)_3(SiBu^tPh_2)_2]^-$ (**3a**, **3b**) or in $(Me_2N)_3M-SiBu^tPh_2$ (**11a**, **11b**) to give $M(NMe_2)_4$ (**1a**, **1b**).

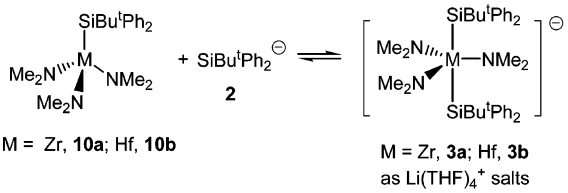

(3)

The amide−silyl exchange involving $(Me_2N)_3Zr-N(SiMe_3)_2$ (**6a**), prepared from $(Me_2N)_3ZrCl$ and $LiN(SiMe_3)_2$ (**7**-Li), and $LiSiBu^tPh_2$ (**2**-Li) has also been investigated. Compound **6a** reacts with **2**-Li to give **3a** and **7**-Li in toluene. This provides an easier, alternative method to prepare **3a**-Li. In THF-d_8, a reversible reaction in eq 4 was observed and the system quickly reached an equilibrium. It is not clear why

(16) In these THF-d_8 solutions, Li^+ cations in **1b**-Li_2 probably exist as free $Li(THF\text{-}d_8)_4^+$ ions. In addition, our current studies of $[Zr(NMe_2)_4]_2$ (**1a**$_2$) in THF-d_8 suggest that it exists as the monomeric adduct $Zr(NMe_2)_4(THF\text{-}d_8)_2$.

(17) See Supporting Information for details.

the substitutions in the forward and reverse reactions are selective. In the forward reaction, the silyl anion **2** *selectively* replaces the $-N(SiMe_3)_2$ ligand in **6a**, affording exclusively $[(Me_2N)_3Zr(SiBu^tPh_2)_2]^-$ (**3a**) and $N(SiMe_3)_2^-$ (**7**). No substitution of the $-NMe_2$ ligand in $(Me_2N)_3Zr-N(SiMe_3)_2$ (**6a**) was observed. In the reverse reaction, amide anion $-N(SiMe_3)_2^-$ (**7**) replaces the silyl ligands in **3a**. It is interesting to note that, in the reverse reaction, the amide anion $-N(SiMe_3)_2^-$ (**7**) did not replace the $-NMe_2$ ligand in $[Zr(NMe_2)_3(SiBu^tPh_2)_2]^-$ (**3a**). In the ^{1}H EXSY spectrum of a mixture of **2** and **6a** at 32 °C,[17] cross-peaks were observed between $-NMe_2$, $-SiBu^tPh_2$, and $-N(SiMe_3)_2$ peaks, respectively, indicating an exchange process involving the complexes in eq 4. Thermodynamic studies of this equilibrium by ^{1}H NMR spectroscopy were conducted.

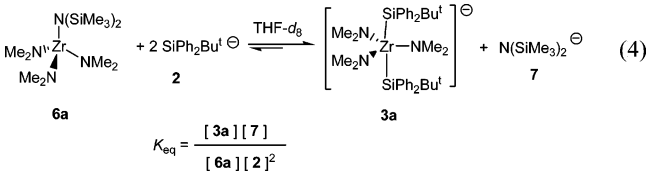

(4)

The equilibrium constants K_{eq} (Table 3) range from 10.0(1) at 223 K to 3.77(5) at 303 K. The forward reaction in eq 4, the selective substitution of the $-N(SiMe_3)_2$ ligand in **6a** by $(SiBu^tPh_2)^-$ (**2**), is slightly favored, and lowering the temperature shifts the equilibrium in eq 4 to the products side. The plot of ln K_{eq} versus $1000/T$ gives the thermodynamic parameters for this equilibrium:[17] $\Delta H° = -1.61(12)$ kcal/mol, $\Delta S° = -2.6(5)$ eu, and $\Delta G°_{298\ K} = -0.8(2)$ kcal/mol. Although the entropy change $\Delta S°$ [−2.6(5) eu] < 0 in the forward reaction, the enthalpy change [$\Delta H° = -1.61(12)$ kcal/mol] outweighs the entropy change, making the exothermic forward reaction slightly favored.

Amide−Silyl Exchanges Involving the $[Si(SiMe_3)_3]^-$ (8) Anion. When $M(NMe_2)_4$ (**1a**, **1b**) and $(Me_2N)_3M-N(SiMe_3)_2$ (M = Zr, **6a**; Hf, **6b**) were added $Li(THF)_xSi(SiMe_3)_3$ (**8**-Li),[10b] substitution of the amide ligands $-NMe_2$ and $-N(SiMe_3)_2$, respectively, were observed, yielding the monosilyl complexes $(Me_2N)_3M-Si(SiMe_3)_3$ (M = Zr, **9a**; Hf, **9b**).[7f] The reactions are reversible, giving the equilibria in eqs 5 and 6. No disilyl complexes were observed, perhaps as a result of the bulkiness of the $-Si(SiMe_3)_3$ ligand. In contrast to eqs 2 and 3, the *reverse* reactions in eqs 5 and 6 yielding amides **1a** (**1b**) or **6a** (**6b**) and **8**-Li are preferred in the equilibria. In THF-d_8, only ∼6% of **8**-Li converted to $(Me_2N)_3Zr-Si(SiMe_3)_3$ (**9a**) in the equilibrium of the Zr complexes in eq 5, and $K_{eq} = 4.5(9) \times 10^{-3}$ and $\Delta G° = 3.20(13)$ kcal/mol at 298 K. A much more significant conversion (43%) of $Li(THF)_3Si(SiMe_3)_3$ (**8**-Li) to $(Me_2N)_3Hf-Si(SiMe_3)_3$ (**9b**) was observed in the equilibrium of the Hf complexes in eq 5, and $K_{eq} = 3.0(6)$ and $\Delta G° = -0.65(11)$ kcal/mol at 298 K. It is not clear why the Hf complex **1b** undergoes more extensive conversion in its reaction with **7**-Li. For the equilibria involving $(Me_2N)_3M-N(SiMe_3)_2$ (**6a**, **6b**) in eq 6, $K_{eq} = 1.1(1) \times 10^{-2}$ and $1.0(1) \times 10^{-2}$ [$\Delta G° = 2.7(1)$ kcal/mol] at 298 K for the Zr and Hf complexes, respectively. Except for the reaction of **1b** with **8**-Li in eq 5, the formation of silyl complexes $(Me_2N)_3M-Si(SiMe_3)_3$ (**9a**, **9b**) in eqs 5 and 6 is not thermodynamically favored. Cooling the equilibrium mixture of **1b**, **8**, **9b**, and **4b** (eq 5) in toluene-d_8 to −36 °C gave crystals of $(Me_2N)_3Hf-Si(SiMe_3)_3$ (**9b**) in 16.9% yield.

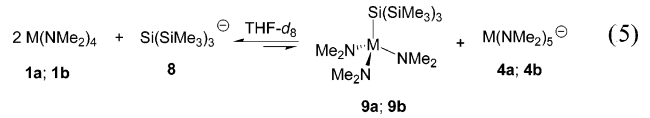

(5)

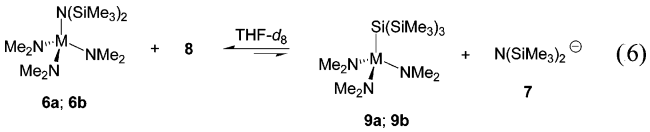

(6)

Preparation and Crystal Structure of $(Me_2N)_3Hf-Si(SiMe_3)_3$ (9b). The crystal structure of the Zr complex $(Me_2N)_3Zr-Si(SiMe_3)_3$ (**9a**) had been reported by our group.[7f] The efforts to make single crystals of its Hf analog **9b** that were suitable for X-ray diffraction were not successful then. In the current work, such crystals of **9b** were prepared from the amide−silyl exchange reaction of $Hf(NMe_2)_4$ (**1b**) with $Li(THF)_2Si(SiMe_3)_3$ (**8**-Li). A molecular drawing, crystallographic data, and selected bond distances and angles of **9b** are given in Figure 2, Table 1, and Table 4, respectively. The crystal structures of **9a** and **9b** are isomorphous. A crystallographically imposed 3-fold rotation axis exists along the Hf−Si bond with three amide ligands on the Hf atom staggered with respect to the trimethylsilyl groups on the tertiary Si atom. The one Hf and three Si atoms all exhibit a pseudotetrahedral geometry with angles between 106.22(18) and 113.8(4)°. The Hf−N bond distance of 2.017-

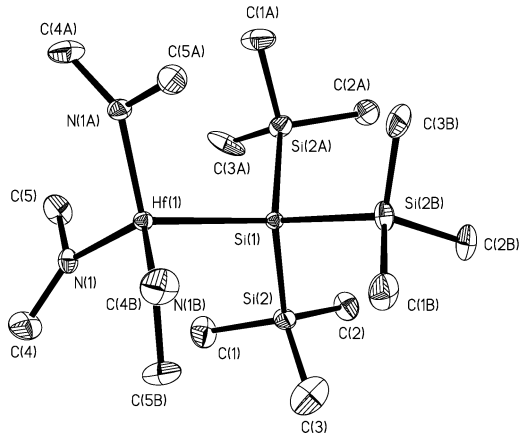

Figure 2. Molecular drawing of **9b** showing 30% probability thermal ellipsoids. Hydrogen atoms are omitted for clarity.

Table 4. Selected Bond Distances (Å) and Angles (deg) for **9b**

Hf(1)−N(1)	2.017(8)	C(5)−N(1)	1.425(14)
Hf(1)−Si(1)	2.743(6)	C(1)−Si(2)	1.874(12)
Si(1)−Si(2)	2.332(4)	C(2)−Si(2)	1.859(11)
C(4)−N(1)	1.435(14)	C(3)−Si(2)	1.754(15)
N(1)−Hf(1)−N(1A)	111.7(2)	Si(2)−Si(1)−Si(2B)	106.22(18)
N(1)−Hf(1)−Si(1)	107.1(3)	Si(2)−Si(1)−Hf(1)	112.55(16)
C(5)−N(1)−C(4)	112.5(9)	C(3)−Si(2)−Si(1)	109.1(4)
C(5)−N(1)−Hf(1)	110.1(7)	C(2)−Si(2)−Si(1)	113.8(4)
C(4)−N(1)−Hf(1)	137.4(8)	C(1)−Si(2)−Si(1)	110.0(4)

(8) Å is close to the Zr−N distance of 2.018(7) Å in **9a**. The Hf−Si bond distance of 2.743(6) Å is shorter than the Zr−Si distance of 2.784(4) Å in **9a**. It is similar to the distances of 2.748(4) Å in $Cp^*C1_2Hf-Si(SiMe_3)_3$[18a] and 2.744(1) Å in $Cp^*CpHf[SiH(SiMe_3)_2]H$[18b] but is shorter than distances of 2.802(6) Å in $Cl_3Hf[Si(SiMe_3)_3](Me_2NCH_2CH_2NMe_2)$,[18c] 2.863(2) Å in chelating K(18-crown-6)$_{3/2}\{(Me_2N)_3Hf[\eta^2\text{-}(Me_3Si)_2Si(CH_2)_2Si(SiMe_3)_2]\}$ (**12b**),[7n] and 2.896(7)−2.918(7) Å in $[Li(THF)_4][(Me_2N)_3Hf(SiBu^tPh_2)_2]$ (**3b**-Li).[7n]

Reactions of $Zr(NMe_2)_4$ (1a) and $(Me_2N)_3M-N(SiMe_3)_2$ (6a, 6b) with $[K(18\text{-crown-}6)]_2[(Me_3Si)_2Si(CH_2)_2Si(SiMe_3)_2]$ (13-K_2). When $Zr(NMe_2)_4$ (**1a**) was added with 1 equiv of **13**-K_2 in benzene-d_6, the formation of K(18-crown-6)$_{3/2}\{(Me_2N)_3Zr[\eta^2\text{-}(Me_3Si)_2Si(CH_2)_2Si(SiMe_3)_2]\}$ (**12a**) was observed (eq 7), and the reaction was completed in ∼10 min. No reverse reaction was observed. Compound **12a** has been prepared earlier through the reaction of $(Me_2N)_3Zr-Cl$ with **13**-K_2.[7n] It is interesting to note that there is no sign of **1a** in the mixture. This observation suggests that, unlike the equilibrium involving $Li(THF)_2SiBu^tPh_2$ (**2**-Li) and the disilyl complexes $[(Me_2N)_3M(SiBu^tPh_2)_2]^-$ (**3a**,**3b**; eq 2), the substitution of amide ligands in $Zr(NMe_2)_4$ (**1a**) by chelating $[(Me_3Si)_2Si(CH_2)_2Si(SiMe_3)_2]^{2-}$ (**13**) is *irreversible*. This is perhaps not surprising because the substitution of monodentate ligands by chelating ligands is in part driven thermodynamically by entropy increase.[19]

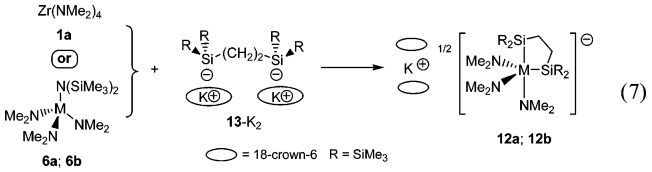

(7)

A similar reaction between $(Me_2N)_3M-N(SiMe_3)_2$ (**6a**, **6b**) and $[K(18\text{-crown-}6)]_2[(Me_3Si)_2Si(CH_2)_2Si(SiMe_3)_2]$ (**13**-K_2) in benzene-d_6 was also investigated by using a 1:1 molar ratio of the reagents. The ^1H NMR spectrum of the reaction mixture showed that both **6** and **13**-K_2 gradually disappeared with the formation of K(18-crown-6)$_{3/2}\{(Me_2N)_3M[\eta^2\text{-}(Me_3Si)_2Si(CH_2)_2Si(SiMe_3)_2]\}$ (**12a**, **12b**) in 21−24 h. Compared to the reaction of $Zr(NMe_2)_4$ (**1a**) with **13**-K_2, **6a** (or **6b**) and **13**-K_2 were found to react much more slowly. The bulkiness of $(Me_2N)_3Zr-N(SiMe_3)_2$ (**6a**) in comparison to $Zr(NMe_2)_4$ (**1a**) probably contributes to its slow reactions.

X-ray Crystal Structure of $[Hf(NMe_2)_4]_2$ (Dimer of 1b). In the course of the current studies of the amide−silyl exchanges involving **1b**, crystals of $[Hf(NMe_2)_4]_2$ were obtained from crystallization in toluene, and its structure was solved. A molecular drawing, crystallographic data, and selected bond distances and angles of $[Hf(NMe_2)_4]_2$ are given in Figure 3, Table 1, and Table 5, respectively. In the solid state, $Hf(NMe_2)_4$ (**1b**) adopts a dimeric structure, like its Zr analog, which Chisholm and co-workers reported earlier.[9a] In the structure of $[Hf(NMe_2)_4]_2$, the local coordination around each Hf atom is square pyramidal, and the dimerization of the two $Hf(NMe_2)_4$ units occurs by the fusing of square pyramids along a common equatorial edge. In $[Hf(NMe_2)_4]_2$, the local coordination about each Zr atom corresponds to a distorted trigonal bipyramid (TBP).[9a] The two Zr and the two bridging N atoms in $[Zr(NMe_2)_4]_2$ form a centrosymmetric, planar parallelogram core, and the six terminal $-NMe_2$ ligands are in a staggered conformation (C_{2h} symmetry). In contrast, the two Hf and bridging N atoms in $[Hf(NMe_2)_4]_2$ form a nonplanar core with six terminal $-NMe_2$ ligands in an eclipsed conformation (C_{2v} symmetry). The bridging Hf−N bond distances of 2.262(7)−2.324(7) Å are longer than the terminal Hf−N bond distances of 2.028(7)−2.074(8) Å.

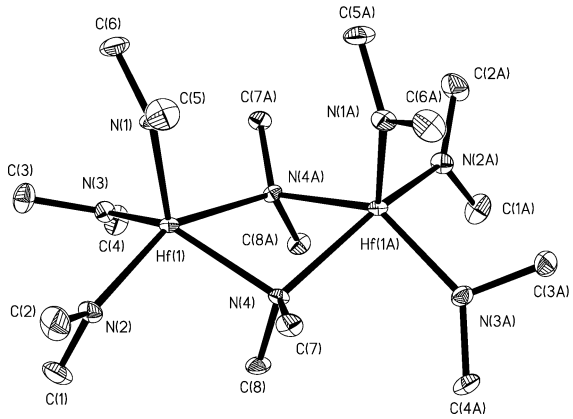

Figure 3. Molecular drawing of $[Hf(NMe_2)_4]_2$ showing 30% probability thermal ellipsoids. Hydrogen atoms are omitted for clarity.

Table 5. Selected Bond Distances (Å) and Angles (deg) for $[Hf(NMe_2)_4]_2$

Hf(1)−N(1)	2.028(7)	Hf(1)−N(3)	2.064(6)
Hf(1)−N(2)	2.074(8)	Hf(1)−N(4)	2.262(7)
Hf(1)−N(4A)	2.324(7)		
N(1)−Hf(1)−N(3)	106.1(3)	N(1)−Hf(1)−N(2)	104.6(2)
N(3)−Hf(1)−N(2)	94.1(3)	N(1)−Hf(1)−N(4)	111.6(2)
N(3)−Hf(1)−N(4)	139.7(3)	N(2)−Hf(1)−N(4)	90.0(3)
N(1)−Hf(1)−N(4A)	102.9(2)	N(3)−Hf(1)−N(4A)	87.4(3)
N(2)−Hf(1)−N(4A)	150.9(3)	N(4)−Hf(1)−N(4A)	71.0(3)

In the current work, several equilibria involving amide−silyl exchanges are reported. It is interesting that amide ligands in d^0 complexes are replaced by silyl anions, and the reactions are reversible. Although many mechanistic studies have been performed on ligand exchange reactions of late-transition-metal complexes,[20] there are few such studies involving a d^0 metal center. Thermodynamic studies of the equilibria in the current systems have been conducted. These systems also provide a unique opportunity to understand nucleophilic substitution reactions that are commonly used in synthetic chemistry.

(18) (a) Arnold, J.; Roddick, D. M.; Tilley, T. D.; Rheingold, A. L.**;** Geib, S. J. *Inorg. Chem.* **1988**, *27*, 3510. (b) Casty, G. L.; Lugmair, C. G.; Radu, N. S.; Tilley, T. D.; Walzer, J. F.; Zargarian, D. *Organometallics* **1997**, *16*, 8. (c) Frank, D.; Baumgartner, J.; Marschner, C. *Chem. Commun.* **2002**, 1190.

(19) $KNMe_2$ is believed to be a product in the reaction in eq 7. It was prepared from the reaction of $PhCH_2K$ with $HNMe_2$.[18] $KNMe_2$ was found to be pyrophoric and unstable in benzene-d_6 and THF-d_8, decomposing to unknown species. Its formation in this reaction (eq 7) could thus not be confirmed.

(20) (a) Crabtree, R. H. *The Organometallic Chemistry of the Transition Metals*; Wiley: New York, 1994. (b) Wilkinson, R. G. *Kinetics and Mechanism of Reactions of Transition Metal Complexes*; VCH: New York, 1991. (c) Jordan, R. B. *Reaction Mechanism of Inorganic and Organometallic Systems*; Oxford University Press: New York, 1991.

Experimental Section

General Procedures. All manipulations were performed under a dry nitrogen atmosphere with the use of either a dry box or standard Schlenk techniques. Solvents were purified by distillation from potassium/benzophenone ketyl. Benzene-d_6, THF-d_8, and toluene-d_8 were dried over activated molecular sieves and stored under N_2. The freezing point depression experiment was conducted in benzene. MCl_4 (M = Zr, Hf) was freshly sublimed prior to use. $Li(THF)_xSiBu^tPh_2$ (**2**-Li, x = 2, 3)[10a] and $Li(THF)_xSi(SiMe_3)_3$ (**8**-Li, x = 2, 3)[10b] were prepared by the literature procedures. $M(NMe_2)_4$ (**1a**, **1b**) were prepared from MCl_4 and 4 equiv of $LiNMe_2$ in hexanes[8,9] and were crystallized from toluene at −30 °C. ^1H and $^{13}C\{^1H\}$ NMR spectra were recorded on a Bruker AC-250, Bruker AMX-400, or Varian Mercury 300 spectrometer and referenced to solvent (residual protons in the ^1H spectra). ^1H EXSY (exchange spectroscopy) spectrum was recorded at 32 °C on the Bruker AMX-400 spectrometer. Elemental analyses were performed by Complete Analysis Laboratories Inc., Parsippany, New Jersey.

In the thermodynamic studies, the equilibrium constants K_{eq} were obtained from at least two separate experiments at a given temperature, and their averages are listed. The concentrations of the species involved in the equilibria were determined from the ^1H NMR spectra. The estimated uncertainty in the temperature measurements for an NMR probe was 1 K. The enthalpy ($\Delta H°$) and entropy ($\Delta S°$) were calculated from an unweighted nonlinear least-squares procedure. The uncertainties in $\Delta H°$ and $\Delta S°$ were computed from the following error propagation formulas which were derived from $-RT \ln K_{eq} = \Delta H° - T\Delta S°$:[7e]

$$(\sigma\Delta H°)^2 = \frac{R^2(T_{min}{}^4T_{max}{}^2 + T_{min}{}^2T_{max}{}^4}{(T_{max} - T_{min})^4} \times \left[\ln\left(\frac{K_{eq(max)}}{K_{eq(min)}}\right)\right]^2\left(\frac{\sigma T}{T}\right)^2 + \frac{2R^2T_{max}{}^2T_{min}{}^2}{(T_{max} - T_{min})^2}\left(\frac{\sigma K_{eq}}{K_{eq}}\right)^2 \quad (8)$$

$$(\sigma\Delta S°)^2 = \frac{2R^2T_{min}{}^2T_{max}{}^2}{(T_{max} - T_{min})^4} \times \left[\ln\left(\frac{K_{eq(max)}}{K_{eq(min)}}\right)\right]^2\left(\frac{\sigma T}{T}\right)^2 + \frac{R^2(T_{max}{}^2 + T_{min}{}^2)}{(T_{max} - T_{min})^2}\left(\frac{\sigma K_{eq}}{K_{eq}}\right)^2 \quad (9)$$

Preparation of $[(Me_2N)_3Zr(SiBu^tPh_2)_2]^-[Zr(NMe_2)_5Li_2(THF)_4]^+$ (5). Freshly sublimed $Zr(NMe_2)_4$ (**1a**, 300 mg, 1.12 mmol) was mixed with $Li(THF)_2SiBu^tPh_2$ (**2**-Li, 394 mg, 1.08 mmol) in a Schlenk flask. Cold toluene (−10 °C, ∼4 mL) was added to the mixture to dissolve the two compounds. The solution was then cooled to −30 °C in a cold bath. Bright orange crystals gradually grew from the solution. The crystals were washed four times by cold toluene (2 mL per wash). Stripping away all volatiles afforded a yellow crystalline solid of **5** (407 mg, 0.309 mmol, 55.2% based on **1a**). Anal. Calcd for $C_{64}H_{118}N_8O_4Si_2Zr_2Li_2$: C, 58.40; H, 9.04. Found: C, 58.27; H, 8.91.

The equilibrium in eq 2 was observed when **5** was dissolved in THF-d_8. ^1H NMR (THF-d_8, 400.0 MHz, 25 °C): δ 7.49, 6.97, 6.87 (m, Ph), 3.62 (m, THF), 2.90 (s, −N*Me*$_2$, **1a**), 2.82 (s, −N*Me*$_2$, **4a**), 2.75 (s, −N*Me*$_2$, **3a**), 1.77 (m, THF), 0.950 (s, −C*Me*$_3$, **2**), 0.862 (s, −C*Me*$_3$, **3a**). $^{13}C\{^1H\}$ NMR (THF-d_8, 100.6 MHz, 25 °C): δ 137.59, 126.46, 124.41 (Ph), 68.23 (THF), 44.75 (−N*Me*$_2$, **4a**), 43.43 (−N*Me*$_2$, **3a**), 43.14 (−N*Me*$_2$, **1a**), 31.87 (-*Bu*^{t}, **2**-Li), 31.48 (−C*Me*$_3$, **3a**), 27.87 (−*C*Me$_3$, **3a**), 26.36 (THF).

Preparation of $(Me_2N)_3Zr-N(SiMe_3)_2$ (6a). $LiNMe_2$ (3.29 g, 64.5 mmol) in THF (40 mL) at −30 °C was added dropwise to a slurry of $ZrCl_4$ (5.00 g, 21.5 mmol) in THF (30 mL) at −30 °C. The mixture was warmed with stirring to room temperature overnight and was then cooled to −30 °C. $LiN(SiMe_3)_2$ (3.59 g, 21.5 mmol, **7**-Li) in THF (30 mL) at −30 °C was added slowly. After the mixture was stirred overnight, all volatiles were removed in vacuo. Hexanes (2 × 40 mL) were added, and the solution was filtered. A solid was obtained after the volatiles in the filtrate were removed in vacuo. Sublimation in vacuo at 60 °C gave a white waxy solid of **6a** (6.20 g, 16.2 mmol, 75.1% yield). ^1H NMR (benzene-d_6, 400.0 MHz, 23 °C): δ 2.90 (s, 18H, N*Me*$_2$), 0.275 (s, 18H, Si*Me*$_3$). $^{13}C\{^1H\}$ NMR (benzene-d_6, 100.6 MHz, 23 °C): δ 42.14 (N*Me*$_2$), 4.38 (Si*Me*$_3$). ^1H NMR (THF-d_8, 400.0 MHz, 23 °C) δ 2.94 (s, 18H, N*Me*$_2$), 0.170 (s, 18H, Si*Me*$_3$). $^{13}C\{^1H\}$ (THF-d_8, 100.6 MHz, 23 °C): δ 42.59 (N*Me*$_2$), 4.55 (Si*Me*$_3$). Anal. Calcd for $C_{12}H_{36}N_4Si_2Zr$: C, 37.55; H, 9.45. Found: C, 37.31; H, 9.28.

Preparation of $(Me_2N)_3Hf-N(SiMe_3)_2$ (6b). $LiNMe_2$ (2.39 g, 46.8 mmol) in THF (30 mL) at −40 °C was added dropwise to a slurry of $HfCl_4$ (5.00 g, 15.6 mmol) in THF (30 mL) at −40 °C. The mixture was warmed with stirring to room temperature overnight. The mixture was then cooled to −30 °C, and $LiN(SiMe_3)_2$ (2.61 g, 15.6 mmol) in THF (30 mL) at −30 °C was added slowly. After the mixture was stirred overnight, all volatiles were removed in vacuo. Hexanes (2 × 30 mL) were added, and the solution was filtered. A solid was obtained after the volatiles in the filtrate were removed in vacuo. Sublimation in vacuo at 55 °C gave a white waxy solid of **6b** (5.75 g, 12.2 mmol, 78.2% yield). ^1H NMR (benzene-d_6, 400.0 MHz, 23 °C): δ 2.93 (s, 18H, N*Me*$_2$), 0.288 (s, 18H, Si*Me*$_3$). $^{13}C\{^1H\}$ NMR (benzene-d_6, 100.6 MHz, 23 °C): δ 41.69 (N*Me*$_2$), 4.43 (Si*Me*$_3$). ^1H NMR (THF-d_8, 400.0 MHz, 23 °C): δ 2.93 (s, 18H, N*Me*$_2$), 0.157 (s, 18H, Si*Me*$_3$). $^{13}C\{^1H\}$ (THF-d_8, 100.6 MHz, 23 °C): δ 42.05 (N*Me*$_2$), 4.53 (Si*Me*$_3$). Anal. Calcd for $C_{12}H_{36}N_4Si_2Hf$: C, 30.59; H, 7.70. Found: C, 30.31; H, 7.59.

Preparation of $(Me_2N)_3Hf-Si(SiMe_3)_3$ (9b). $Li(THF)_3Si(SiMe_3)_3$ (**8**-Li, 47.0 mg, 0.118 mmol) and $Hf(NMe_2)_4$ (**1b**, 42.0 mg, 0.118 mmol) were weighted in a Young's NMR tube. Toluene-d_8 (∼0.45 mL) was added. Colorless crystals of **9b** (11.2 mg, 0.0200 mmol, 33.9% yield based on **1b**) formed at −36 °C. ^1H NMR (benzene-d_6, 250.1 MHz, 23 °C): δ 2.94 (s, 18H, N*Me*$_2$), 0.39 (s, 27H, Si*Me*$_3$). $^{13}C\{^1H\}$ NMR (benzene-d_6, 62.5 MHz, 23 °C): δ 38.9 (N*Me*$_2$), 5.2 (Si*Me*$_3$). $^{29}Si\{^1H\}$ NMR (DEPT, benzene-d_6, 79.5 MHz, 23 °C): δ −2.1 (*Si*Me$_3$), −103.5 [*Si*(SiMe$_3$)$_3$]. Anal. Calcd for $C_{15}H_{45}N_3Si_4Hf$: C, 32.27; H, 8.12. Found: C, 32.12; H, 8.12.

Thermodynamic Studies of the Equilibrium in Equation 2. In the first experiment, $Zr(NMe_2)_4$ (**1a**, 22.2 mg, 0.0830 mmol), $Li(THF)_2SiBu^tPh_2$ (**2**-Li, 26.8 mg, 0.0686 mmol) and 4,4′-dimethyl biphenyl (internal standard, 11.4 mg, 0.0625 mmol) were added to THF-d_8 (0.428 mL) in a Young's NMR tube. In the second experiment, $Zr(NMe_2)_4$ (**1a**, 34.5 mg, 0.129 mmol), **2**-Li (56.7 mg, 0.145 mmol), and 4,4′-dimethyl biphenyl (15.1 mg, 0.0828 mmol) were added to THF-d_8 (0.528 mL) in a Young's NMR tube. Another solution was prepared by dissolution of $[(Me_2N)_3Zr(SiBu^tPh_2)_2]^-[Zr(NMe_2)_5Li_2(THF)_4]^+$ (**5**, 20.5 mg, 0.0156 mmol) and 4,4′-dimethyl biphenyl (15.1 mg, 0.0828 mmol) in THF-d_8 (0.472 mL). Variable-temperature ^1H NMR studies of these three solutions were carried out between 308 and 243 K.

Similar thermodynamic studies were conducted involving $Hf(NMe_2)_4$ (**1b**, 30.8 mg, 0.0868 mmol) and $Li(THF)_2SiBu^tPh_2$ (**2**-Li, 40.3 mg, 0.103 mmol). The mixture was added to 4,4′-dimethyl biphenyl (internal standard, 11.7 mg, 0.0642 mmol) and dissolved in THF-d_8 (0.432 mL). Variable-temperature ^1H NMR studies of these three solutions were carried out between 308 and 243 K.

In toluene-d_8, an equilibrium involving $Zr(NMe_2)_4$ (**1a**), $SiBu^tPh_2^-$ (**2**), **3a**, **4a**, and $Zr(NMe_2)_6^{2-}$ (**10**) was observed. The ^1H NMR peaks of the amide ligands ($-NMe_2$) in **3a**, **4a**, **1**, and **10** were severely overlapped, preventing accurate quantitative studies of the equilibrium.

Thermodynamic Studies of the Equilibrium in Equation 4. In the first experiment, $(Me_2N)_3Zr-N(SiMe_3)_2$ (**6a**, 39.4 mg, 0.103 mmol), $Li(THF)_2SiBu^tPh_2$ (**2**-Li, 74.9 mg, 0.192 mmol) and the internal standard 4,4′-dimethyl biphenyl (23.5 mg, 0.129 mmol) were added to THF-d_8 (0.719 mL) in a Young's NMR tube. In the second experiment, **6a** (21.1 mg, 0.549 mmol), **2**-Li (41.8 mg, 0.107 mmol), and 4,4′-dimethyl biphenyl (14.8 mg, 0.0812 mmol) were added to THF-d_8 (0.524 mL) in a Young's NMR tube. The VT-NMR studies were conducted between 303 and 223 K.

Thermodynamic Studies of the Equilibrium in Equations 5 and 6. For the equilibrium of the Zr complexes in eq 5, $Zr(NMe_2)_4$ (**1a**, 41.9 mg, 0.157 mmol), $Li(THF)_2Si(SiMe_3)_3$ (**8**-Li, 36.4 mg, 0.0913 mmol), and 4,4′-dimethyl biphenyl (12.5 mg, 0.0686 mmol) were mixed and added to THF-d_8 (0.527 mL). The ^1H NMR spectrum at 298 K was used to give K_{eq}. Similar studies were performed using $Hf(NMe_2)_4$ (**1b**, 31.2 mg, 0.0879 mmol), $Li(THF)_3Si(SiMe_3)_3$ (**8**-Li, 20.8 mg, 0.0450 mmol), 4,4′-dimethyl biphenyl (6.0 mg, 0.033 mmol), and THF-d_8 (0.488 mL).

For the equilibrium of the Zr complexes in eq 6, $(Me_2N)_3Zr-N(SiMe_3)_2$ (**6a**, 38.7 mg, 0.101 mmol) and $Li(THF)_3Si(SiMe_3)_3$ (**8**-Li, 48.0 mg, 0.102 mmol) were added to THF-d_8 (0.557 mL). The ^1H NMR spectrum at 298 K was used to give K_{eq}. No internal standard was used for the calculation of K_{eq}. Similar thermodynamic studies were conducted for the Hf analogs.

Freezing Point Depression Studies of a Solution of $[(Me_2N)_3Zr(SiBu^tPh_2)_2]^-[Zr(NMe_2)_5Li_2(THF)_4]^+$ (5) in Benzene. The solubility of **5** in cyclohexane was found too small for freezing point depression studies. Complex **5** (363 mg, 0.276 mmol) was dissolved in benzene (4.043 g). The melting point of the solution was measured with a digital thermometer. The measurement was repeated two more times. The melting point decreased from 5.49 to 4.43 °C. From the freezing point depression equation ($K_f = 5.12$ °C/m), $\Delta T_f = -iK_fm$, $i = 3.03$.

Reaction of $Zr(NMe_2)_4$ (1a) with $[K(18\text{-crown-}6)]_2[(Me_3Si)_2Si(CH_2)_2Si(SiMe_3)_2]$ (13-K_2). Compounds **1a** (27.3 mg, 0.102 mmol) and **13**-K_2 (100 mg, 0.102 mmol) in an NMR tube were added to benzene-d_6 at 23 °C. The ^1H NMR spectrum was taken in 10 min. The spectrum revealed that the peak of **1a** had disappeared.

Reactions of $(Me_2N)_3M-N(SiMe_3)_2$ (6a, 6b) with $[K(18\text{-crown-}6)]_2[(Me_3Si)_2Si(CH_2)_2Si(SiMe_3)_2]$ (13-K_2). Compounds **6b** (48.1 mg, 0.102 mmol) and **13**-K_2 (100 mg, 0.102 mmol) in an NMR tube were added to benzene-d_6 at 23 °C. ^1H NMR spectra were taken in a few minutes and the next day. After 1 day, the ^1H NMR peaks of **6b** had disappeared. Similar studies were conducted involving $(Me_2N)_3Zr-N(SiMe_3)_2$ (**6a**) and **13**-K_2.

Determination of X-ray Structures of 5, 9b, and $[Hf(NMe_2)_4]_2$. The data for the X-ray crystal structures of **5**, **9b**, and $[Hf(NMe_2)_4]_2$ were collected on a Bruker AXS Smart 1000 X-ray diffractometer equipped with a CCD area detector and a graphite-monochromated Mo source (Kα radiation, 0.71073 Å) and fitted with an upgraded Nicolet LT-2 low-temperature device. A suitable crystal was coated with paratone oil (Exxon) and mounted on a hairloop under a stream of nitrogen at −100(2) °C. The structure of **5** was first solved by direct methods in the triclinic space group $P\bar{1}$ and then converted to its correct monoclinic space group $C2/c$, while structures of **9b** and $[Hf(NMe_2)_4]_2$ were solved by direct methods. Non-hydrogen atoms were anistropically refined. All hydrogen atoms were treated as idealized contributions. Empirical absorption correction was performed with SADABS.[21] In addition, the global refinements for the unit cells and data reductions of the two structures were performed using the SAINT program (version 6.02). All calculations were performed using the SHELXTL (version 5.1) proprietary software package.[21] A close look of the residue peak of 2.792 e $Å^{-3}$ in the electron density map of **9b** showed it was only 1.13 Å to a Si atom, indicating it is a result of the relatively poor crystal quality, not unsolved atoms/solvent molecules.

Acknowledgment. The authors thank the National Science Foundation, Camille Dreyfus Teacher-Scholar program, and the Ziegler Research Fund for support of the research. The authors thank Prof. Zhenyang Lin's research group and Prof. Charles E. Strouse for helpful discussions.

Supporting Information Available: Preparation of $KNMe_2$, NMR assignments for $Zr(NMe_2)_5^-$ (**4a**) in THF-d_8, observation of $Zr(NMe_2)_4(THF)_2$ in toluene-d_8, EXSY spectra of the exchanges in eqs 2 and 4, ln K_{eq} versus 1000/T plots, and crystallographic data for **5**, **9b**, and $[Hf(NMe_2)_4]_2$. This material is available free of charge via the Internet at http://pubs.acs.org.

IC7010293

(21) (a) Sheldrick, G. M. *SADABS, A Program for Empirical Absorption Correction of Area Detector Data*; University of Göttingen: Göttingen, Germany, 2000. (b) Sheldrick, G. M. *SHELXL-97, A Program for the Refinement of Crystal Structures*; University of Göttingen: Göttingen, Germany, 1997.